Adsorption and corrosion inhibitive properties of novel surfactants in the series of fatty acids based on palm oil on carbon steel in CO_2-containing solution

I. T. Ismayilov[a, b], Hany M. Abd El-Lateef[a, c]*, V. M. Abbasov[a], L. I. Aliyeva[a], E. N. Efremenko[b], S. A. Mamedxanova[a]

[a] *Mamedaliev Institute of Petrochemical Processes, National Academy of Sciences of Azerbaijan, AZ1025 Baku, Azerbaijan*

[b] *Faculty of Chemistry, Lomonosov Moscow State University, 119991, GSP-1, 1-3 Leninskiye Gory, Moscow, Russia*

[c] *Chemistry Department, Faculty of Science, Sohag University, 82524 Sohag, Egypt*

E-mail address: *Hany_shubra@yahoo.co.uk*

Authors' contributions

"This work was carried out in collaboration between all authors. All authors contributed in practical work and managed the analysis of the study. All authors read and approved the final manuscript."

ABSTRACT

Some novel surfactants in the series of fatty acids were synthesized based on palm oil. The inhibition efficiency (η %) of these surfactants has been studied by both linear polarization corrosion rate and potentiodynamic polarization measurements in CO_2-saturated brine at 50 ℃. A significant decrease in the corro sion rate was observed in the presence of the investigated inhibitors. The percentage inhibition efficiency (η%) increases by increasing the inhibitor concentration. Potentiostatic polarization curves indicate that, the inhibitors under investigation act as mixed type. Tafel slopes are approximately constant and independent on the inhibitor concentration. The observed corrosion data indicate that, the inhibition of carbon steel corrosion is due to the adsorption of the inhibitor molecules on the surface, which follow Langmuir adsorption isotherm. The surface morphology of carbon steel samples in absence and presence of the inhibitor was examined using Energy dispersive X-ray fluorescence (EDRF).

KEYWORDS: *Carbon steel, palm oil, surfactants, inhibition, EDRF*

1. INTRODUCTION

A wide range of liquids is extracted from oil and gas fields to meet the energy demands of the world. In addition to these liquids, compounds such as carbon dioxide, water and hydrogen sulphide are present naturally in gas wells. Carbon dioxide which is present naturally is also injected purposely into gas wells to enhance oil recovery. These compounds combine to form a corrosive environment under different environmental conditions such as temperature, pressure, pH and concentration. Carbon dioxide (CO_2) corrosion, also known as "sweet corrosion" is one of the major problems in oil and gas industry, costing billions of dollars every year **[1]**. In CO_2 corrosion, CO_2 dissolves and hydrates to form carbonic acid (H_2CO_3), which then dissociates into bicarbonate, carbonate and hydrogen ions **[2-8]**. Due to its low cost and availability, carbon steel is used as the primary construction material for pipelines in oil and gas industries, but it is very susceptible to corrosion in CO_2 environments. Aqueous carbon dioxide (carbonic acid) is corrosive and corrodes the carbon

steel pipelines. Carbon dioxide corrosion has been of interest to researchers in oil industries for many years and there exists many theories about the mechanism of CO_2 corrosion **[9, 10].**

Corrosion inhibitors are used to prevent metal dissolution as well as acid consumption **[11].** Most organic inhibitors are substances with at least one functional group, which considered as the reaction center for the adsorption process. The adsorption of inhibitors is related to the presence of heteroatom as nitrogen [12], phosphorus and sulfur [13, 14]. Surfactants are special type of organic compounds and exhibit unique properties due to their amphiphilic molecule. This is the reason of their wide application in the field of inhibition of metals against corrosion. A molecular layer of surfactants is formed as a result of this attraction with the construction of a hydrophobic barrier, which prevent the contact of the metal surface with the environment. The surfactant inhibitors have many advantages such as high inhibition efficiency, low price, low toxicity and easy production [**15–17].** The adsorption of the surfactant on the metal surface can markedly change the corrosion-resisting property of the metal [18], and so the study of the relationship between the adsorption and corrosion inhibition is of great importance.

The aim of this study is to investigate the adsorption and corrosion inhibitive properties of newly synthesized surfactants in the series of fatty acids on carbon steel in CO_2 containing solution using linear polarization corrosion rate and potentiodynamic polarization and Energy dispersive X-ray fluorescence techniques.

2. MATERIALS AND METHODS

2.1. Chemical composition of carbon steel alloy

Electrodes are made of carbon steel grade 080A15 and have an area of 4.55 cm^2. The Chemical composition of low carbon steel used in this study was given in Table **1**. The data was provided by European Corrosion Supplies Ltd.

Table 1: Chemical composition of low carbon steel alloy.

Element	Si	Ni	Cr	C	S	P	Mn	Fe
Content, (wt. %)	0.24	0.01	0.10	0.18	0.05	0.05	0.50	Balance

2.2. Synthesis of Surfactants

Palm oil was reacted with diethanolamine for 7 hours at 150-160 ℃. These processes produce fatty acid diethanolamine amide. Based on the last prepared compound sulfating syntheses were performed**.** The product is **s**ulfated fatty acid diethanolamine amide. Six types from surfactants were synthesized in high purity by the following compositions: [$R\text{-}CH\text{-}(OSO_3M)\text{-}CON\text{-}(CH_2\text{-}CH_2\text{-}OH)_2$] (where M= Na, K, NH_4, $–NH\text{-}CH_2\text{-}CH_2\text{-}OH$, $–N\text{-}(CH_2\text{-}CH_2\text{-}OH)_2$ and $–N(CH_3)_2$). List of the synthesized surfactants are shown in Table **2**.

2.3. Preparation of solutions

The aggressive solution, 1% NaCl, was prepared by dissolving of analytical grade NaCl in distilled water. The concentration range of the prepared surfactants was from 25 to 100 ppm used for corrosion measurements. All inhibitors solutions were prepared using a mixture from distilled water and alcohol in a different ratio.

2.4. Corrosion measurements

The measurements were performed on the rotating cylinder electrode. This electrode was used for one time. The reference electrode was Ag/AgCl Electrode to which all potentials are referred.

Before beginning the experiment, the prepared 1% - of sodium chloride solution was stirred by a magnetic stirrer for 60 min in 1000 ml cell. Then this cell was thermostated at a temperature 50 º C for 1 hour under a pressure of 0.9 bars. The solution was saturated with carbon dioxide. To remove any surface contamination and air formed oxide, the working electrode was kept at−1500 mV (Ag/AgCl) for 5 min in the tested solution, disconnected shaken free of adsorbed hydrogen bubbles and then cathodic and anodic polarization was

recorded. ACM Gill AC instrument connected with a personal computer was used for the measurements.

2.4.1. Potentiodynamic polarization measurements

The extrapolation of cathodic and anodic Tafel lines was carried out in a potential range ±100 mV with respect to corrosion potential (E_{corr}) at scan rate of 1 mV/s.

2.4.2. Linear polarization resistance corrosion rate

The LPR method is ideal for plant monitoring offering an almost instantaneous indication of corrosion rate, allowing for quick evaluation of remedial action and minimizing unscheduled downtime. The prepared 1% - of the solution sodium chloride was stirred by a magnetic stirrer for 60 min in 4000 ml. The prepared solution poured into the 4 glass beakers (1000 ml for each one). Then these beakers were placed on a heater at 50 º C for 1 hour under a pressure of 0.9 bars. The solution was saturated with carbon dioxide. After that, the electrodes were placed in the medium and are connected through a potentiometer ACM GILL AC. The surface of working electrode is cleaned by acetone before using, these electrodes are using for one time. After 1 hour, except for 1 beaker, the remaining 3 is fed with the suitable amount of inhibitor and continued supply of CO_2 under pressure of 0.9 bar until the end of the experiment.

The potential of the working electrode was varied by a CoreRunning programme (Version 5.1.3.) through an ACM instrument Gill AC. The CoreRunning programme converts a corrosion current in mA/cm^2 to a corrosion rate in mm/year. A cylindrical carbon steel rod of the composition 080A15 GRADE STEEL was used as a working electrode. Gill AC technology allows measure DC and AC signals using standard Sequencer software. A small sweep from typically –10 mV to +10 mV at 10 mV/min around the rest potential is performed.

2.5. Surface characterization

In order to observe any changes in surface morphologies of the carbon steel samples after testing, the specimens were first immersed in the test media with and without an inhibitor for 3 days, then cleaned with bi-distilled water and acetone, and dried with cool air. Then the morphology of the tested sample was observed by using HORIBA XGT-7000 - Energy dispersive X-ray fluorescence (EDRF), a microscope with a system of partial / complete evacuation of the sample.

2.6. Methods of evaluation of corrosion parameters

Steady state of open circuit corrosion potential (E_{corr}) for the investigated electrode in the absence and presence of the studied inhibitor was attained after 50–60 min from the moment of immersion. Corrosion current density (I_{corr}) of the investigated electrodes was determined [**19]**, by extrapolation of cathodic and anodic Tafel lines to corrosion potential (E_{corr}). The inhibition efficiency expressed as percent inhibition (η%) is defined as:

$$\eta\% = \frac{I_{uninh.} - I_{inh.}}{I_{uninh.}} \times 100 \qquad (1)$$

where $I_{uninh.}$ and $I_{inh.}$ are the uninhibited and inhibited corrosion currents. The inhibited corrosion currents are those determined in the presence of the studied surfactants used in this investigation. The uninhibited corrosion currents were determined in pure (inhibitor free) CO_2-saturated 1% NaCl solution at the same temperature.

Table 2: List of the synthesized surfactants includes, code number, name and structure.

Code number of the inhibitor	Name and abbreviation	Structure	molecular weight (g /mol)
I	Sodium salt of sulfated fatty acid diethanolamine amide (**SS**)	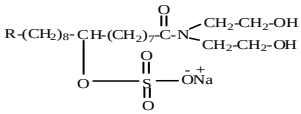	438
II	Potassium salt of **s**ulfated fatty acid diethanolamine amide (**PS**)	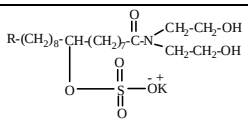	454
III	Ammonium salt of **s**ulfated fatty acid diethanolamine amide (**AS**)	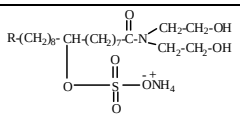	432
IV	Sulfated fatty acid diethanolamine amide- monoethanolamine complex (**MC**)	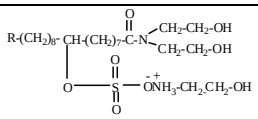	465
V	Sulfated fatty acid diethanolamine amide- diethanolamine Complex (**DC**)	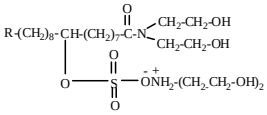	513
VI	Sulfated fatty acid diethanolamine amide- dimethylamine Complex (**DM**)	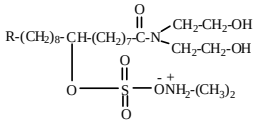	465

3. RESULTS AND DISCUSSIONS

3.1 LPR corrosion rate and corrosion potential

LPR test has been performed in brine saturated with CO_2 at 50 ℃, in turbulence fluid stream during 20 hours. Figure **1** shows that, the change in corrosion rate (CR) with time for carbon steel in CO_2-saturated 1%NaCl solution containing different concentrations form inhibitors (a) **II**, (b) **VI** and (c) **V** at 50 ℃. The inhibitor was added after 1 hour of exposure because at this time the corrosion potential got stable, allowing the measurement of the CR prior the injection of the inhibitor. The initial corrosion rate, without inhibitor, was measured to be between 3.45 and 5.03 mm y^{-1}, but in the presence 100 ppm of the investigated inhibitors between 0.154 and 0.031 mm y^{-1}. It can be observed from Figure **1** that, the CR, in the absence of inhibitor, tends to increase with time. The increase in CR has been attributed to the galvanic effect between the ferrite phase and cementite (Fe_3C) which is a part of the original steel in the non-oxidized state and accumulates on the surface after the preferential dissolution of ferrite (α-Fe) into Fe^{2+} **[20]**. Fe_3C is known to be less active than the ferrite phase. Therefore, there is a preferential dissolution of ferrite

over cementite, working the former as the anode and latter as the cathode, favoring the hydrogen evolved reaction (HER) during the corrosion process **[21, 22].**

Variation of the corrosion rate for inhibitors **II**, **VI** and **V** at different concentrations are presented in Figure **1**. Corrosion parameters were calculated on the basis of LPR corrosion rate test. The inhibition efficiency (η %) and surface coverage (θ) were calculated according to the following equations:

$$\eta\% = \frac{CR_0 - CR_i}{CR_0} \times 100 \quad (2)$$

$$\text{Surface coverage}(\theta) = \theta = 1 - \frac{CR_i}{CR_0} \quad (3)$$

where CR_o is the corrosion rate without inhibitor and CR_i is the corrosion rate when inhibitor is present. It can be seen that the presence of inhibitors results a high decrease in the rate of corrosion. In the case of these inhibitors, the corrosion rate decreases as the inhibitor concentration increases, getting maximum inhibition efficiency ranged between 97.00 and 99.90 % at 100 ppm after 20 hour of exposure (Table **3**). This trend may results from the fact that adsorption and surface coverage increase with the increase in concentration; thus the surface is effectively separated from the medium [**23]**.

Table **3** shows the calculated values of corrosion rates, the inhibition efficiencies and the surface coverage in the absence and presence of different concentrations of different inhibitors at 50 ℃. The data exhibited that, the c orrosion rates, the inhibition efficiencies and the surface coverage are found to depend on the concentrations of the inhibitors. The corrosion rate (CR) are decreased, and the inhibition efficiencies (η%) and the surface coverage (θ) are increased with the increase of the surfactant concentrations. This indicates that the inhibitory action of the inhibitors against carbon steel corrosion can be attributed to the adsorption of these molecules on the metal surface, limits the dissolution of carbon steel, and the adsorption amounts of surfactants on carbon steel increase with concentrations in the corrosive solutions.

Figure **2** shows the variation of the corrosion rate with time for carbon steel in CO_2-saturated brine containing 100 ppm from different surfactants at 50 ℃. This plot indicates that, the presence of different inhibitors decreases the rate of corrosion. However, the maximum decrease in the corrosion rate was observed for inhibitor (**V**) and the inhibition efficiency of the investigated surfactants was increased in the following order: **V>IV>II>VI>III>I**. The highest inhibition efficiency of inhibitors **IV** and **V** may be attributed to the following reasons:

I. The higher electron density on the functional groups leads to easier bond formation, greater adsorption, and consequently, higher inhibition **[24].**

The high inhibition efficiency obtained in CO_2- saturated solution in the presence of studied inhibitors by all investigated methods can be attributed to the formation of a protective film of iron carbonate ($FeCO_3$) as follows **[25]:**

$$CO_{2(g)} \leftrightarrow CO_{2(aq)} \quad (4)$$

$$CO_{2(aq)} + H_2O \leftrightarrow H_2CO_{3(aq)} \quad (5)$$

$$H_2CO_{3(aq)} \leftrightarrow H^+ + HCO_3^- \quad (6)$$

$$HCO_3^- \leftrightarrow H^+ + CO_3^{2-} \quad (7)$$

The anodic dissolution for iron in carbonic acid solutions gives ferrous ions **[25]**.

$$Fe \leftrightarrow Fe^{2+} + 2e^- \quad (8)$$

According to these processes, a corrosion layer was formed on the steel surface. The properties of the formed layers and its effect on the corrosion rate are important factors to take into account when studying the corrosion of steels in CO_2 environments. Ogundele and White suggested that, iron carbonate, $FeCO_3$, may be important in the formation of

protective layers on steel surface **[26]**. The formation of iron carbonate can be explained by using the following Eq**. [27]**.

$$Fe^{2+} + CO_3^{2-} \rightarrow FeCO_3 \quad (9)$$

Figure 3 shows the change in corrosion potential (E_{corr}) with time for carbon steel in CO_2-saturated brine in the absence and presence of inhibitor (**V**). It can be observed, an anodic shift in E_{corr} that is characteristic of anodic and anodic/cathodic inhibitor **[28].** It was explained that this shift in E_{corr} is due to active sites blocking effect that occurs when an inhibitor is added **[29].** In the case of CO_2 corrosion the anodic a cathodic reactions are the oxidation of iron and the reduction of hydrogen, respectively **[30].** If it is considered that the active sites on the metal surface are the same for both reactions before adding the inhibitor, it is logical the change in E_{corr} when the inhibitor is present because its adsorption change those active sites and therefore the anodic and cathodic reaction rates. Another important aspect is that the change in E_{corr} is proportional to the inhibitor efficiency. Higher efficiencies were observed when the change in E_{corr} was toward more noble values **[18].**

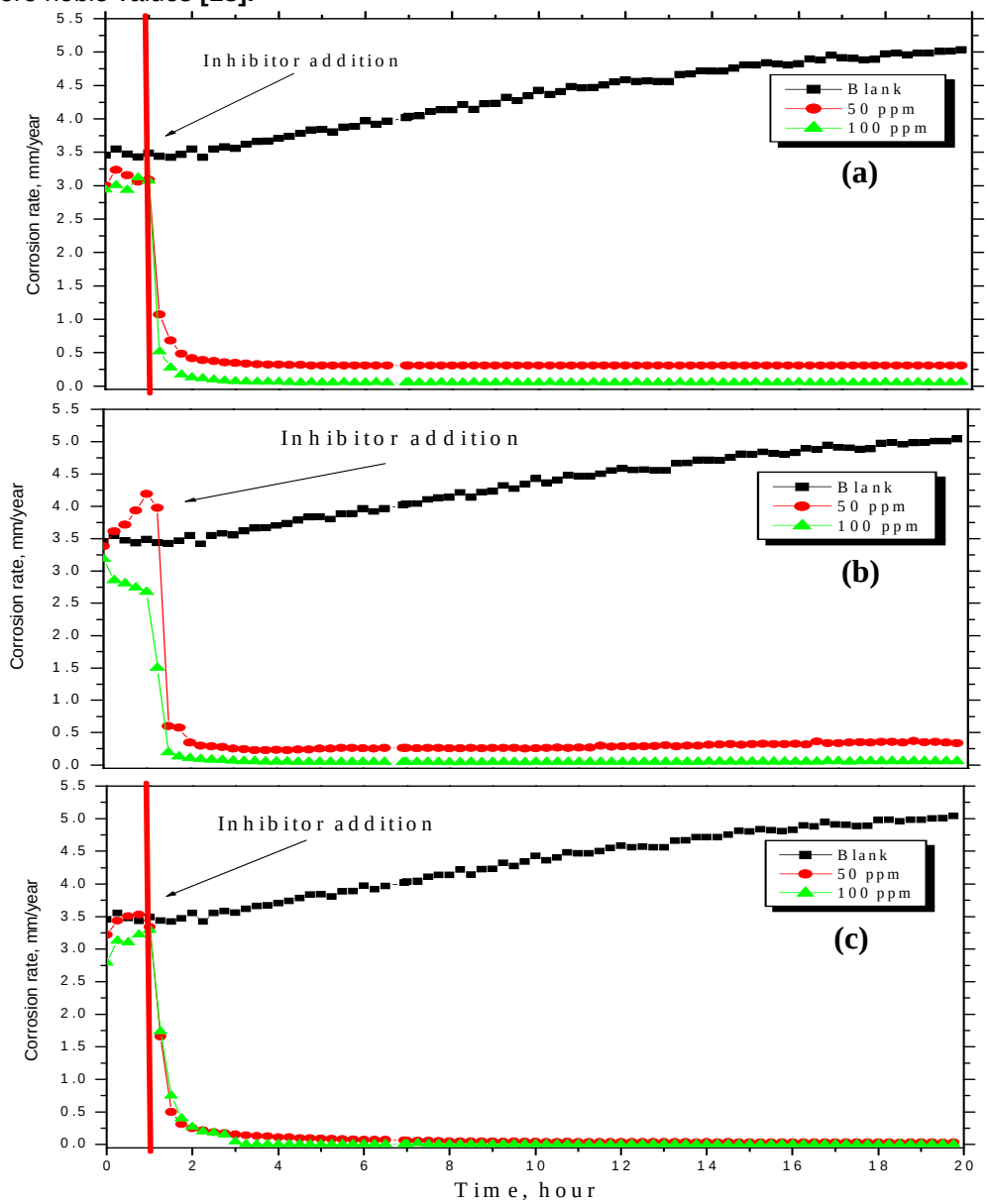

Figure 1: Variation of the Corrosion rate with time for mild steel in CO_2-saturated 1 % NaCl solution containing different concentrations of inhibitors (a) II, (b) VI and (c) V based on palm oil at 50 ℃.

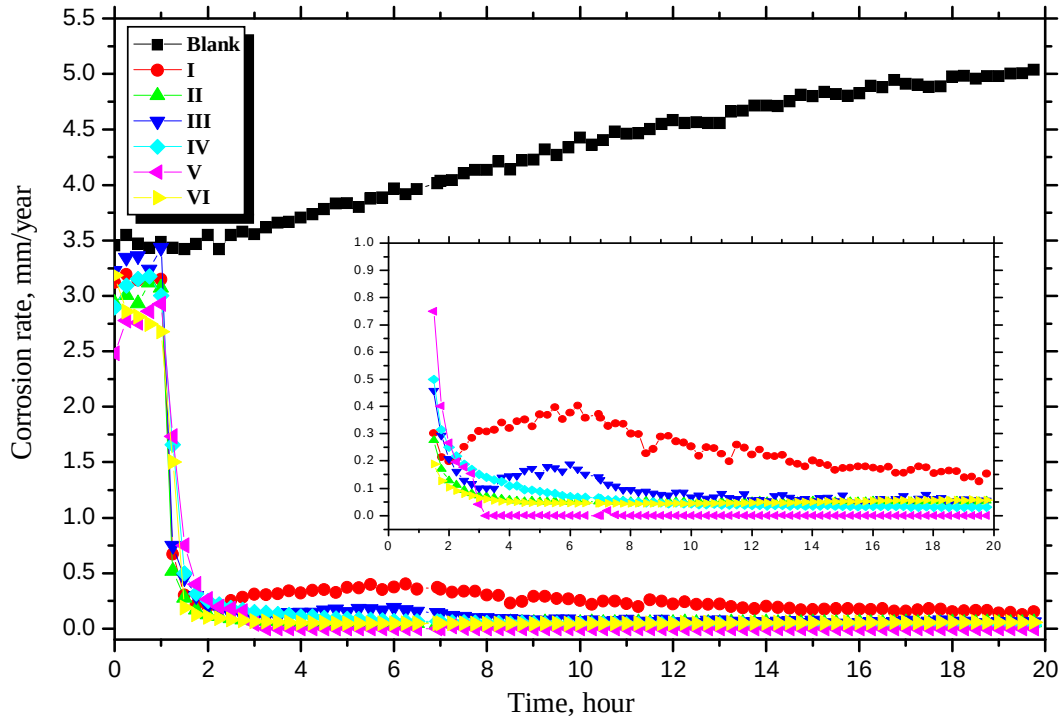

Figure 2: Variation of the Corrosion rate with time for carbon steel in CO_2-saturated 1% NaCl solution containing 100 ppm of different inhibitors at 50 ℃.

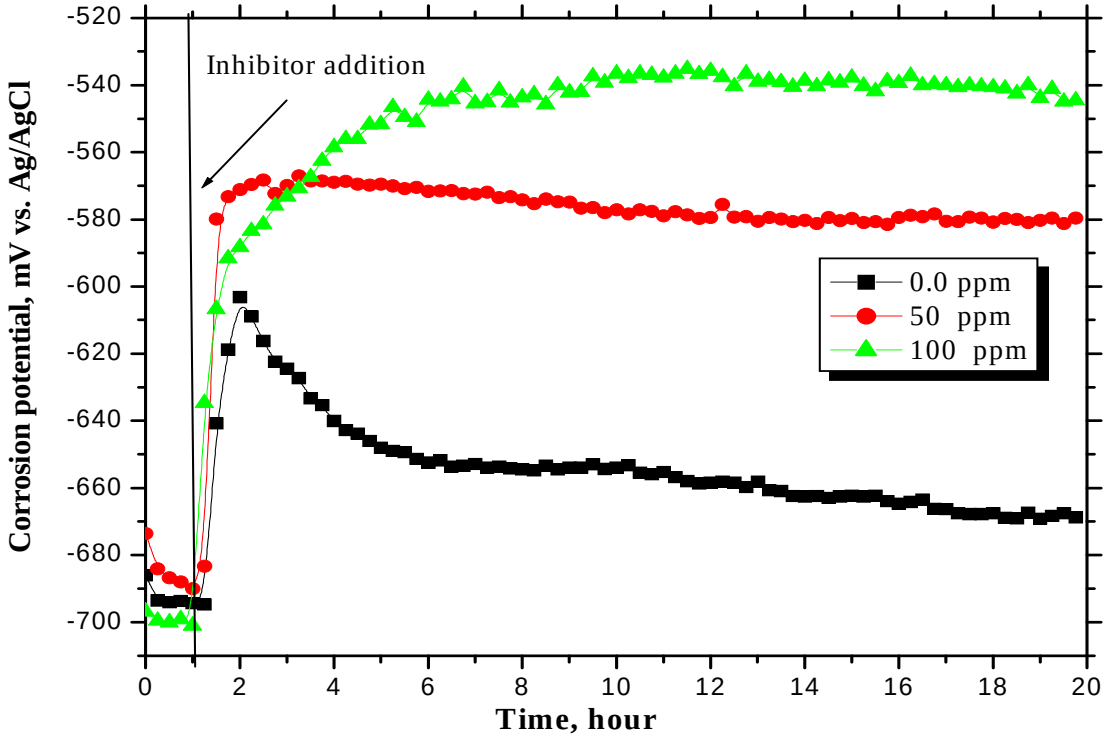

Figure 3: Change in corrosion potential vs. time for carbon steel in CO_2-saturated 1 % NaCl solution containing different concentrations from inhibitor V.

Table 3: The corrosion parameters obtained from LPR corrosion rate measurements for carbon steel electrode in CO_2-saturated brine in the absence and presence of various concentrations of investigated surfactants at 50 ℃.

Inhibitors code	Concentration, ppm	Corrosion rate (mm/year)	Surface coverage θ	The inhibition efficiency, η%
Absence	0.0	5.037	-----	-----
I	50	0.497	0.90	90.12
	100	0.154	0.97	97.00
II	50	0.308	0.93	93.88
	100	0.054	0.98	98.92
III	50	0.426	0.91	91.54
	100	0.056	0.98	98.88
IV	50	0.178	0.96	96.45
	100	0.031	0.99	99.40
V	50	0.031	0.99	99.38
	100	0.005	0.99	99.90
VI	50	0.336	0.93	93.32
	100	0.055	0.98	98.89

3.2. Potentiodynamic polarization measurements

The representative potentiodynamic polarization curves of carbon steel in CO_2-saturated 1.0 % NaCl solution in the absence and presence of various concentrations of inhibitor **V** is shown in Fig. 4. Corrosion parameters were calculated on the basis of cathodic and anodic potential versus current density characteristics in the Tafel potential region. The values of the corrosion current density (I_{corr}) for the investigated metal without and with the inhibitor were determined by the extrapolation of cathodic and anodic Tafel lines to the corrosion potential (E_{corr}). Herein, the corrosion rates were calculated assuming that the whole surface of carbon steel is attacked by corrosion and no local corrosion is observed. The corrosion rates CR (mm year^{-1}) from polarization were calculated using the following equation.

$$CR = \frac{I_{corr} \times t \times M}{F \times S \times d} \times 10 \qquad (10)$$

where t is the time (s), M is the equivalent molar weight of iron (g mol^{-1}), F is Faraday constant (96500 Cmol^{-1}), S is the surface area of electrode, d is the density of iron, the constant 10 is used to convert the unit cm to mm.

As it can be clearly seen from Fig. **4** that, the addition of **DC** to the corrosive solution both reduces anodic dissolution of iron and also retards cathodic hydrogen evolution reactions as would be expected. The corrosion current density as well as corrosion rate of steel considerably reduced in the presence of the inhibitor. These results are indicative of

the adsorption of inhibitor molecules on the carbon steel surface. The inhibition of both anodic and cathodic reactions is more and more pronounced with the increasing inhibitor concentration while the corrosion potential nearly remained the same in comparison with corrosion potential observed in blank solution. These results suggest that **DC** can be classified as the mixed type corrosion inhibitor **[31].** The similar behavior was observed after the addition of other surfactants to the CO_2-saturated solution. It is also obvious that **DC** has higher inhibition efficiency than the other inhibitors at a specified inhibitor concentration.

The electrochemical parameters, I_{corr}, inhibition efficiency (η %), anodic and cathodic Tafel slopes (β_a , β_c) obtained from the polarization measurements were listed in Table **4**. The data exhibited that, the corrosion current density (I_{corr}) decreases, and the inhibition efficiency (η %) increases as the concentration of inhibitors is increased. These results suggest that retardation of the electrodes processes occurs, at both cathodic and anodic sites, as a result of coverage of these sites by surfactants molecules. However, the maximum decrease in I_{corr} was observed for (**V**). This may be attributed to the increase of the electron densities and the molecular size **[32].**The increase of inhibitor efficiency with increasing the concentration can be interpreted on the basis of the adsorption amount and the coverage of surfactants molecules, increases with increasing concentration **[33]**.

The fact that the slopes of the cathodic (β_c) and anodic (β_a) Tafel lines in Table **4** are approximately constant and independent of inhibitor concentration. These results indicate that this inhibitors act by simply blocking the available surface area. In other words, the inhibitor decreases the surface area for corrosion of the investigated metal, and only causes inactivation of a part of the surface with respect to corrosive medium **[32].** On the other hand, the cathodic Tafel slopes (β_c) are also found to be greater than the respective anodic Tafel slopes (β_a). These observations are correlated with the fact that the anodic exchange-current density values are less than those of the cathodic counter parts. It can be concluded that the overall kinetics of corrosion of carbon steel alloy in CO_2 saturated solution are under cathodic control **[19, 23].**

Data in Table **4** shows that the inhibition efficiency increased with increasing the inhibitor concentrations. The inhibition efficiency of the investigated surfactants was increased in the following order: **V>IV>II>VI>III>I**. There was an increase in the efficiency of corrosion inhibition with increasing concentration, since the adsorption of C=O, oxygen, nitrogen and sulfur groups onto the metal surface was stronger, and effectively protecting the surface. Conclusively, the surfactant inhibitor, having near unity θ (Table 4), was considered as a good physical barrier shielding the corroding surface from corrosive medium and dumping the corrosion rate of carbon steel significantly. The inhibition efficiencies are in a good agreement with that calculated from LPR corrosion rate measurements.

The inhibition of carbon steel is attributed to the adsorption of surfactant molecules on the steel surface by the hydrophilic head groups. The hydrophobic chain may be oriented towards the aqueous medium and may be arranged horizontally to the steel surface.

Table 4: Corrosion parameters obtained from Tafel polarization for carbon steel in CO_2-saturted 1% NaCl solution in the absence and presence of different concentrations of the prepared surfactants at 50 ℃ .

Inhibitors Code	Conc. of inhibitor (ppm)	I_{corr} ($mAcm^{-2}$)	β_a ($mVdec^{-1}$)	CR (mm/year)	$-\beta_c$ ($mVdec^{-1}$)	θ	η%
Absence	0.0	0.389	44	4.65	107	---	---
I	25	0.072	47	0.869	103	0.82	81.3
	50	0.044	39	0.534	105	0.86	88.5
	75	0.038	41	0.460	110	0.89	90.1
	100	0.016	44	0.199	108	0.97	95.7
II	25	0.052	42	0.627	107	0.84	86.5
	50	0.031	42	0.376	102	0.87	91.9
	75	0.014	46	0.172	106	0.91	96.3
	100	0.008	41	0.102	111	0.97	97.8
III	25	0.063	42	0.762	108	0.81	83.6
	50	0.038	48	0.460	106	0.85	90.1
	75	0.026	42	0.320	105	0.89	93.1
	100	0.010	40	0.130	102	0.97	97.2
IV	25	0.049	49	0.590	103	0.79	87.3
	50	0.021	46	0.251	110	0.84	94.6
	75	0.011	44	0.134	108	0.89	97.1
	100	0.004	40	0.055	107	0.95	98.8
V	25	0.041	39	0.497	103	0.67	89.3
	50	0.012	41	0.153	100	0.74	96.7
	75	0.009	44	0.111	103	0.82	97.6
	100	0.003	46	0.046	101	0.91	99.0
VI	25	0.057	46	0.688	105	0.73	85.2
	50	0.032	45	0.390	102	0.78	91.6
	75	0.023	41	0.283	103	0.84	93.9
	100	0.010	38	0.120	110	0.92	97.4

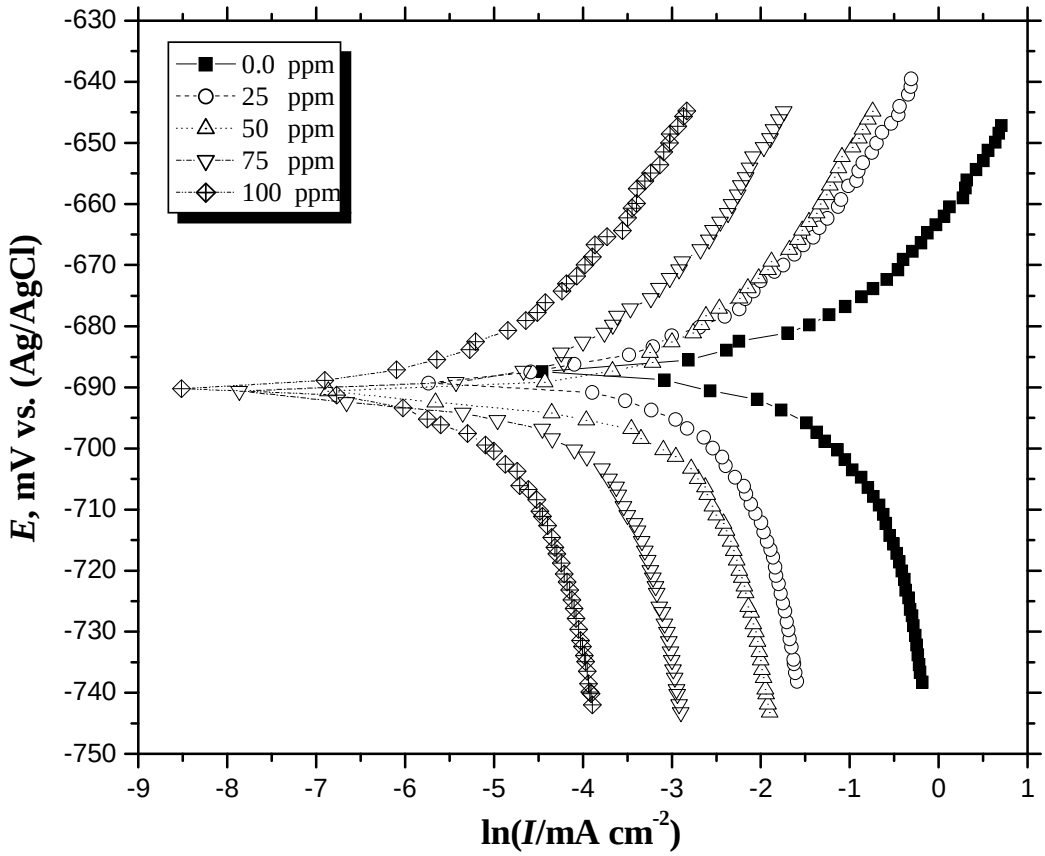

Figure 4: Polarization plots of carbon steel electrode obtained in CO_2-saturated brine containing different concentration of inhibitor (V) at 50 ℃

3.3. Adsorption Isotherm Studies

The degree of surface coverage *(θ)* for different inhibitor concentrations was evaluated from Potentiodynamic polarization measurements**.** The best correlation between the experimental results and isotherm functions was obtained at high inhibitor concentrations using the Langmuir adsorption isotherm. The Langmuir isotherm is given by the following equation **[34]:**

$$\frac{C_{inh}}{\theta} = C_{inh} + \frac{1}{K_{ads}} \tag{11}$$

where K_{ads} is the equilibrium constant of the inhibitor adsorption process and C_{inh} is the surfactant concentration. The plots of C_{inh}/θ vs C_{inh} yielded straight lines with near unit slopes for all the surfactants showing that the adsorption model of these surfactants follows the Langmuir isotherm with good correlation (as shown in Fig.5).

The values of K_{ads} obtained from the Langmuir adsorption isotherm are listed in Table 5, together with the values of the Gibbs free energy of adsorption (ΔG^{o}_{ads}) calculated from **[35]**

$$K_{ads} = \frac{1}{C_{inh}} \times \frac{\theta}{1-\theta} \tag{12}$$

$$\Delta G_{ads} = -2.303RT\log(55.5K_{ads}) \tag{13}$$

Where *R* is the universal gas constant, *T* is the thermodynamic temperature and the value of 55.5 is the concentration of water in the solution.

The high values of K_{ads} for studied surfactants indicate stronger adsorption on the carbon steel surface in CO_2-saturated solution. It is also noted that, the high values of K_{ads} for surfactants **V** and **IV** indicate stronger adsorption on the carbon steel surface than the other surfactants (**I**, **II, III and VI)**. This can be simply explained by the presence of additional donor atoms, such as oxygen, in the appended functional groups. Large values of K_{ads} imply more efficient adsorption and hence better inhibition efficiency **[36]**. The large value of K_{ads} obtained for the studied surfactants agree with the high inhibition efficiency obtained.

Generally, values of ΔG^o_{ads} up to -20 kJ mol^{-1} are consistent with physisorption, while those around -40 kJ mol^{-1} or higher are associated with chemisorption as a result of the sharing or transfer of electrons from organic molecules to the metal surface to form a coordinate bond **[37].** In the present study, The values of ΔG^o_{ads} obtained for studied surfactants on carbon steel in CO_2-saturated solution ranges between -43.58 and -44.86 kJ mol^{-1}, which are more than -40 kJ mol^{-1} (Table **5**). These results indicate that the adsorption mechanism of surfactants on carbon steel in CO_2 saturated solution is typical chemisorption at the studied temperatures. Chemisorption of the surfactant molecules could occur due to the formation of links between the d orbital of iron atoms, involving the displacement of water molecules from the metal surface, and the lone sp^3 electron pairs present on the N, S and/or O atoms of the inhibitor. 1. These results were confirmed by FT-IR. The data for inhibitor **I** (SS) showed that, S=O stretching frequency drops from the level of 1355 cm^{-1} to the level of 1320 cm^{-1}. This suggests that electron cloud of S=O is shifted from S=O up to Fe^{+2} resulting in formation of Fe^{+2} –SS complex on metal surface. The high and negative values obtained for ΔG^o_{ads} indicate that the adsorption process takes place spontaneously by strong interactions between the inhibitor and the steel surface, as was suggested by the obtained values of K_{ads}.

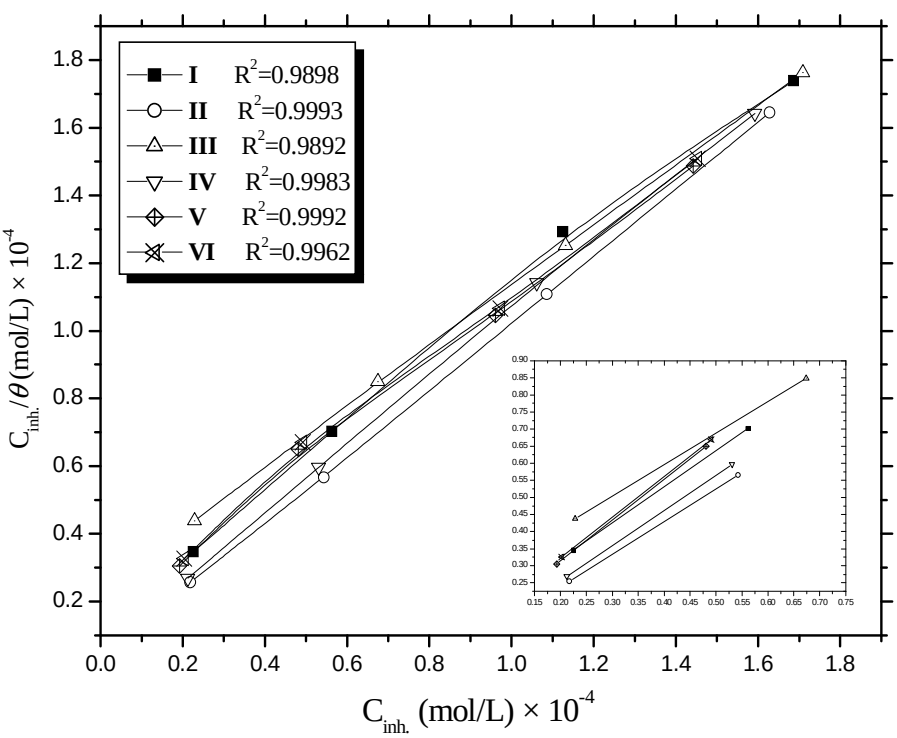

Figure 5: Curve fitting of the corrosion data obtained from Potentiodynamic polarization measurements for carbon steel in CO_2 saturated brine containing various concentrations of inhibitors according to Langmuir adsorption isotherm model at 50 ℃.

Table 5: Thermodynamic parameters for the adsorption of the studied surfactants on carbon steel electrode in CO_2- saturated brine.

Inhibitors Code	Slope	Regression coefficients, R^2	K_{ads}, $M^{-1} \times 10^5$	ΔG^o_{ads} (kJ mol^{-1})
I	1.05	0.9898	2.01	-43.58
II	1.10	0.9993	2.87	-44.54
III	1.05	0.9892	2.23	-43.86
IV	1.04	0.9983	3.23	-44.81
V	1.03	0.9992	3.51	-44.86
VI	1.03	0.9962	2.76	-44.43

3.4. Surface characterization

Figures 6a and 7a show an EDRF spectroscopy for the carbon steel surface after immersed in CO_2-saturated 1% NaCl solution without and with 100 ppm of inhibitor **II** for 3 days. In the absence of inhibitor, Fig. 6a exhibits the characteristics peaks which are related to Fe, Mn, P, Cr and oxygen elements. This indicated that the corrosion product on carbon steel surface being metal oxide and iron carbonate. However, the data in Fig. 7a in the presence of 100 ppm of inhibitor **II** show additional peak characteristic of K element, and the lower peaks height of Fe than those observed in the absence of inhibitors. These results proved that, the adsorption of inhibitor molecule on the carbon steel surface leads to decrease of oxide layer and to isolate the metal surface from the corrosive environment, causing much reduced in the corrosion rates.

The pictures of uninhibited and inhibited carbon steel surfaces are shown Figures 6b and 7b. The morphology of the metal surface immersed in CO_2-saturated brine (Fig. 6b) shows that the surface is rough, covered with corrosion products ($FeCO_3$ layer) and appearing to be full of pits and cavities. The surface was strongly damaged, so that the electrode surface can not be seen. The image of the carbon steel surface after immersion in CO_2-saturated 1% NaCl solution with 100 ppm of inhibitor **II** is shown in Fig. 7b. The presence of the inhibitor leads to the formation of a protective layer adsorbed on the surface, which is responsible for the observed suppression of the rate of corrosion.

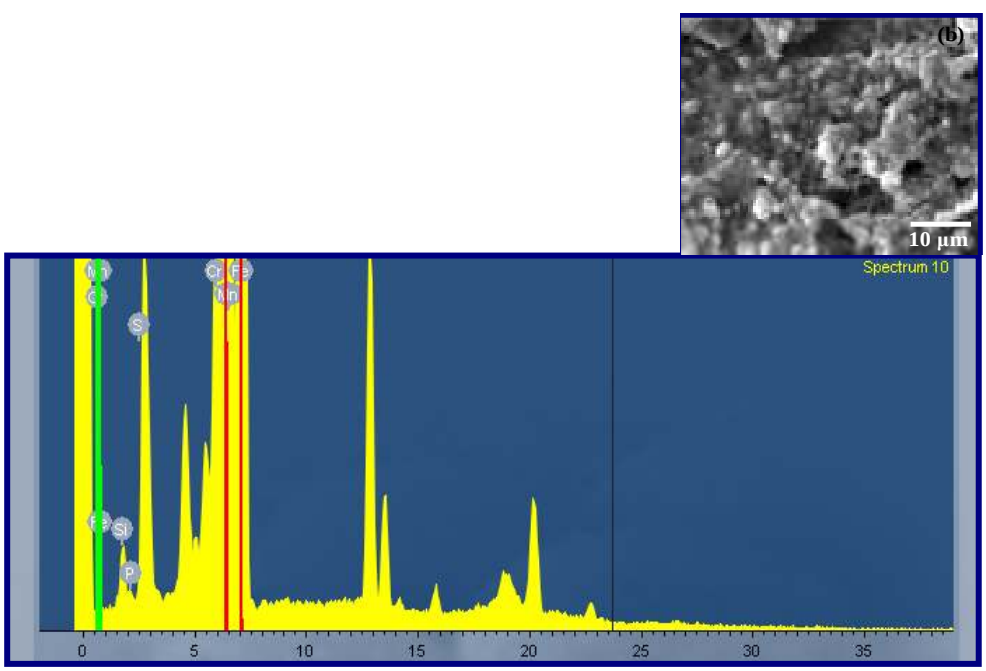

Figure 6: EDRF analysis of carbon steel electrode surface after immersion in CO_2-saturated solution for 3 days without inhibitor (a) and the picture at the same conditions (b).

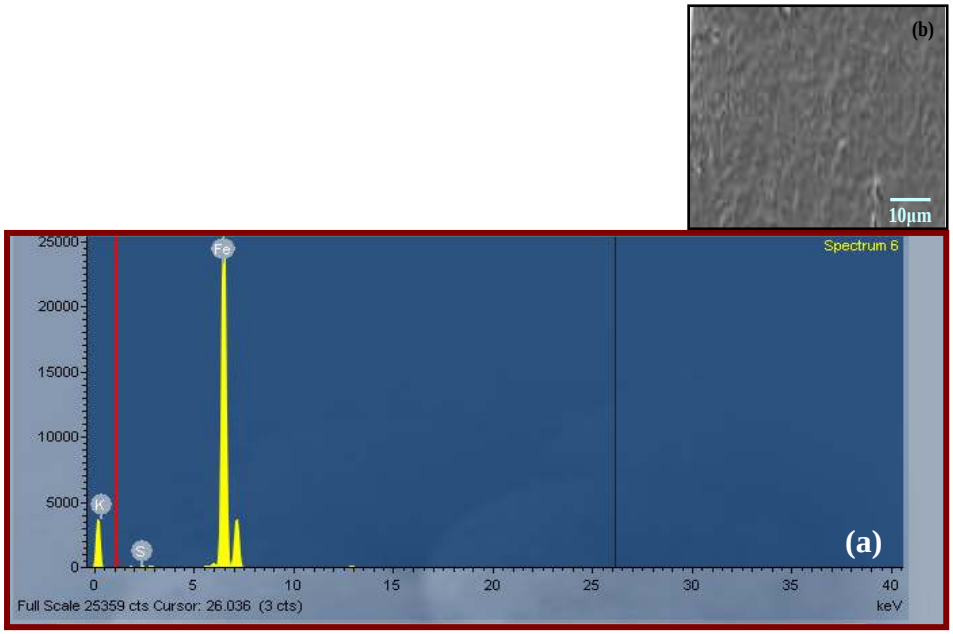

Figure 7: EDRF analysis of carbon steel electrode surface after immersion in CO_2-saturated solution containing 100 ppm of inhibitor II for 3 days (a) and the picture at the same conditions (b).

4. CONCLUSION

In the above results and discussion, the following conclusions are drawn:

1) Novel surfactants in the series of in the series of fatty acids were synthesized based on palm oil and diethanolamine.
2) The corrosion inhibition efficiencies of the synthesized surfactants were studied by linear polarization corrosion rate and Potentiodynamic polarization measurements, and they gave similar results. Test results show that the surfactants studied are efficient inhibitors for carbon corrosion in CO_2-saturated brine solution.
3) The inhibition efficiencies increase with the increase of inhibitor concentrations. The maximum inhibition efficiency was observed for inhibitor **V** (99.90 % at 100 ppm) and the inhibition efficiency of the investigated surfactants was increased in the following order: **V>IV>II>VI>III>I.**
4) The surface coverage θ was calculated on the basis of potentiodynamic polarization measurements and it was found that it can be fitted very well to the Langmuir isotherm.
5) The results of EDRF indicated that, the inhibitor molecules formed a good protective film on the carbon steel surface.

COMPETING INTERESTS

Authors have declared that no competing interests exist.

REFERENCES

1. NACE Corrosion Costs and Preventive Strategies in the United States. http://events.nace.org/publicaffairs/images_cocorr/ccsupp.pdf (15 April 2009),

2. Li, DG, Feng YR, Bai ZQ, Zheng MS. Characteristics of CO_2 Corrosion Scale Formed on N80 Steel in Stratum Water with Saturated CO_2. *Applied Surface Science* 2007**;** 253 (20): 8371-8376.

3. Li T, Yang, Y, Gao K, Lu M. Mechanism of Protective Film Formation During CO2 Corrosion of X65 Pipeline Steel". *Journal of University of Science and Technology Beijing, Mineral, Metallurgy, Material* 2008**;** 15 (6): 702-706.

4. Lopez DA, Simison SN, de Sanchez SR.Inhibitors Performance in CO_2 Corrosion: EIS Studies on the Interaction Between their Molecular Structure and Steel Microstructure. *Corrosion Science* 2005**;** 47 (3): 735-755.

5. Nesic S, Postlethwaite J, Olsen S. An Electrochemical Model for Prediction of Corrosion of Mild Steel in Aqueous Carbon Dioxide Solutions. *Corrosion* 1996**;** 52 (4): 280-294.

6. Sun W, Nesic S. Kinetics of Corrosion Layer Formation: Part 1-Iron Carbonate Layers in Carbon Dioxide Corrosion. *Corrosion* 2008**;** 64 (4): 334-346.

7. Sun W, Nesic S, Papavinasam S. Kinetics of Corrosion Layer Formation. Part 2 - Iron Sulfide and Mixed Iron Sulfide/Carbonate Layers in Carbon Dioxide/Hydrogen Sulfide Corrosion. *Corrosion* 2008**;** 64 (7): 586-599.

8. Wang F.,Postlethwaite J. Modelling of Aqueous CO_2 Corrosion of Iron in Turbulent Pipe Flow, *CORROSION*/2001, paper no. 41 (Houston, TX: NACE, 2001).

9. Bilkova K, Gulbrandsen E. Kinetic and Mechanistic Study of CO_2 Corrosion Inhibition by Cetyl Trimethyl Ammonium Bromide. *Electrochemical Acta* 2008**;** 53 (16): 5423-5433.

10. Dayalan, E.; de Moraes, F. D.; Shadley, J. R.; Shirazi, A.; Rybicki, E. F. "CO_2 Corrosion Prediction in Pipe Flow Under FeCO3 Scale-Forming Conditions", *CORROSION*/1998, paper no. 51 (Houston, TX: NACE, 1998).

11. De Souza FS, Spinelli A., Corros. Sci. 2009; 51: 642.

12. Quraishi MA, Shukla SK, Mater. Chem. Phys. 2009; 113:685.

13. Singh A.K., Quraishi M.A., Corros. Sci. 2009; 51: 2752.

14. Tang YM, Yang WZ, Yin XS, Liu Y, Wan R, Wang JT. Mater. Chem. Phys. 2009; 116: 479.

15. Abbasov V M, Abd El-Lateef HM, Aliyeva LI, Ismayilov IT, Qasimov EE. Efficient Complex Surfactants from the Type of Fatty Acids as Corrosion Inhibitors for Mild Steel C1018 in CO_2-Environments. Journal of the Korean Chemical Society, 2013; 57 (1): 25-34.

16. Abbasov VM, Abd El-Lateef HM, Aliyeva LI, Ismayilov IT. Application of Some Surfactants Based On Corn Oil as Corrosion Inhibitors for Carbon Steel in CO_2 Environments, NACE corrosion 2013, Florida, USA, paper No. 2129: p.1-10.

17. Abd El-Lateef HM, Abbasov VM, Aliyeva LI, Qasimov EE, and Ismayilov IT. LPR Corrosion Rate, Weight Loss Measurements and SEM Studies of the Effect of the Some Novel Surfactants as Corrosion Inhibitors for Carbon Steel in CO_2 -Saturated 1% NaCl Solutions. Journal of Surfaces and Interfaces of Materials 2012; 1: 1–11,.

18. Abd El-Lateef HM, Abbasov VM, Aliyeva LI, Ismayilov TI, Qasimov EE, Ahmadov TU. Novel anionic surfactants based on cottonseed oil and their corrosion inhibition efficiency for carbon steel in CO_2 saturated solution. Global J. Phys. Chem. 2012; 3: 14: 1-12.

19. El-Sayed A, Mohran HS, Abd El-Lateef HM, J. of Power Sources, 2011; 196: 6573–6582.

20. Staicopolus N, J. Electrochem. Soc. 1963; 110: 1121-1124,.

21. Crolet J, Thevenot N, Nesic S, Corrosion, 1998; 54: 194-203.

22. Videm K, Kvarekvaal J, Perez T, Fitzsimons G, NACE Corrosion/96, Houston, Texas, 1996, Paper No. 1.

23. El-Sayed A, Shaker AM, Abd El-Lateef HM. Corrosion inhibition of tin, indium and tin–indium alloys by adenine or adenosine in hydrochloric acid solution. Corros. Sci., 2010; 52: 72-81.

24. Migahed MA, Abd-El-Raouf M, Al-Sabagh AM, Abd-El-Bary HM. Effectiveness of some non ionic surfactants as corrosion inhibitors for carbon steel pipelines in oil fields, Electrochimica Acta 2005; 50: 4683–4689.

25. Damia´n AL, Simison SN, de Sa´nchez SR. The influence of steel microstructure on CO_2 corrosion. EIS studies on the inhibition efficiency of benzimidazole. Electrochimica Acta 2003; 48: 845- 854.

26. Ogundele GI, White WE, Corrosion. 1986; 42 (2): 7.

27. Migahed MA, Abd-El-Raouf M, Al-Sabagh AM, Abd-El-Bary HM, J. Appl. Electrochem., 2006; 36(4): 395,.

28. Cao C, Corr. Sci. 1996; 38: 2073.

29. Nordsveen M, Nesic S, Nyborg R, and Stangelend A, Corrosion 2003; 59: 443.

30. Farelas F, Ramirez A. Carbon Dioxide Corrosion Inhibition of Carbon Steels Through Bis-imidazoline and Imidazoline Compounds Studied by EIS. Int. J. Electrochem. Sci., 2010; 5: 797 – 814.

31. Behpour M, Ghoreishi SM, Soltani N, Salavati-Niasari M. The inhibitive effect of some bis-N, S-bidentate Schiff bases on corrosion behaviour of 304 stainless steel in hydrochloric acid solution, Corros. Sci. 2009; 51: 1073–1082.

32. Akbarzadeh E, Ibrahim MNM, Rahim AA, Int. J. Electrochem. Sci., 2011; 6: 5396 – 5416.

33. El-Sayed A, Mohran HS, Abd El-Lateef HM. Corros. Sci., 2010; 52: 1976–1984.

34. Lebrini M, Traisnel M, Lagrenee M, Mernari B, Bentiss F, Inhibitive properties, adsorption and a theoretical study of 3,5-bis(n-pyridyl)-4-amino-1,2,4-triazoles as corrosion inhibitors for mild steel in perchloric acid. Corros Sci 2008; 50: 473

35. Solmaz R, Kardas G, Culha M, Yazici B, Erbil M, Electrochim. Acta, 2008; 53: 5941.

36. Refay SA, Taha F, Abd El-Malak AM, Appl. Surf. Sci. 2004; 236: 175-185.

37. Szklarska-Smialowska Z, Mankowski J. Crevice corrosion of stainless steels in sodium chloride solution, Corros. Sci. 1978; 18: 953-960.